# Synthesis and Novel Mesomorphic Properties of the Side-Chain Liquid Crystalline Polyacetylenes Containing Phenyl Benzoate Mesogens with Cyano and Methoxy Tails

Xiangxing Kong and Ben Zhong Tang*

*Department of Chemistry and Center for Display Research, Hong Kong University of Science & Technology, Clear Water Bay, Kowloon, Hong Kong, China*

*Received April 30, 1998*

The synthesis of side-chain liquid crystalline polyacetylenes containing phenyl benzoate mesogens with octyl spacers and cyano (**2a**) or methoxy tails (**2b**) is accomplished, and the tuning of the molecular alignments of **2b** is realized by simple mechanical perturbations. The acetylene monomers, 10-[4-(4′-R-phenoxycarbonyl)phenoxycarbonyl]-1-decynes [R = cyano (**1a**), methoxy (**1b**)], are prepared by two consecutive esterification reactions of 10-undecynoic acid. None of the two monomers are liquid crystalline, but **1a** exhibits an unusual crystal−crystal transition at 70.5 °C, probably due to its strong intermolecular ≡C−H···N≡C− hydrogen bonding. The polymerizations of **1** initiated by the $WCl_6$−$Ph_4Sn$/dioxane complex yield yellow powdery polymers (**2**) with $M_w$ of ca. 30 000, whose molecular structures are characterized by NMR, IR, and UV spectroscopy. The mesomorphic behavior of **2** is investigated by DSC, POM, and XRD: **2a** exhibits smecticity in a temperature range as wide as over 100 °C (k 80.4 $s_A$ 194.8 i), while **2b** displays smectic and nematic mesophases in the temperature region of 95−140 °C (k 95.6 $s_A$ 113.9 n 140.8 i). Rotational agitation of the nematic **2b** generates the disclinations of high strengths (*s* up to 2), and translational shear creates the inversion walls, solidification of which produces the well-ordered bands aligned parallel to the shear direction. Such phenomena have not previously been observed in the "conventional" side-chain liquid crystalline polymers with flexible backbones, suggesting that the rigid polyacetylene backbone of **2b** plays an important role in inducing the novel molecular alignments aided by the external mechanical force.

## Introduction

Synthetic polymers are among the most important materials in contemporary society. Most industrial plastics consist of flexible macromolecules, while stiff-chain polymers have been less utilized, partly due to the processing difficulties stemming from their low solubility and high melting temperature.[1,2] Polyethylene [−($CH_2$−$CH_2$)$_n$−], for example, is a flexible macromolecule and a tonnage commodity polymer.[3] In contrast, its counterpart with a rigid alternating-double-bond backbone, i.e., polyacetylene [−(CH=CH)$_n$−], is completely intractable (insoluble and infusible) and has found few, if any, practical applications, notwithstanding the metallic conductivity of its doped form.[4]

In the research community of liquid crystalline polymers, rigid polymer backbones are generally regarded as defects that distort the packing arrangements of mesogenic pendants in side-chain liquid crystalline polymers (SCLCPs). The standard recipe for designing the molecular architecture of a SCLCP given in liquid crystal textbooks is "*flexible* backbone + spacer + mesogenic group".[5] The SCLCPs with flexible backbones have attracted much interest, but those with rigid backbones have received little attention. Compared to the vast variety of the flexible-chain SCLCPs, few of the stiff-chain SCLCPs have been developed and their preparations are often for the purpose of giving comparative examples to demonstrate the destructive roles of the rigid backbones.[5,6] Seldom have any research efforts been actively devoted to the exploration of the constructive roles the rigid backbones may play in inducing novel molecular alignments in the SCLCP systems.

One advantage of the stiff-chain macromolecules over their flexible-chain counterparts is their orientability by external fields and/or flow processes.[2] The stiff

(1) (a) *The Materials Science and Engineering of Rigid-Rod Polymers*; Adams, W. W., Eby, R. K., McLemore, D. E., Eds.; Materials Research Society: Pittsburgh, PA, 1989. (b) Tsvetkov, V. N. *Rigid-Chain Polymers*; Consultants Bureau: New York, 1989.

(2) For a review, see: Ballauff, M. *Angew. Chem., Int. Ed. Engl.* **1989**, *28*, 253.

(3) (a) Saunders, K. J. *Organic Polymer Chemistry*; Chapman & Hall: New York, 1973; Chapter 2. (b) Dyson, R. W. In *Specialty Polymers*; Dyson, R. W., Ed.; Chapman & Hall: New York, 1987; p 1.

(4) (a) Chien, J. C. W. *Polyacetylene*; Academic Press: New York, 1984. (b) Krivoshei, I. V.; Skorobogatov, V. M. *Polyacetylene and Polyarylenes*; Gordon and Breach Science Publishers: New York, 1991. (c) *Conjugated Conducting Polymers*; Kiess, H. G., Ed.; Springer-Verlag: Berlin, 1992.

(5) (a) Cowie, J. M. G. *Polymers: Chemistry & Physics of Modern Materials*, 2nd ed.; Blackie: London, 1991; Chapter 16. (b) McArdle, C. B. *Side Chain Liquid Crystal Polymers*; Blackie: London, 1989.

(6) *Handbook of Liquid Crystal Research*; Collings, P. J., Patel, J. S., Eds.; Oxford University Press: New York, 1997.

10.1021/cm9803152 CCC: $15.00 
Published on Web 10/20/1998

**Scheme 1**

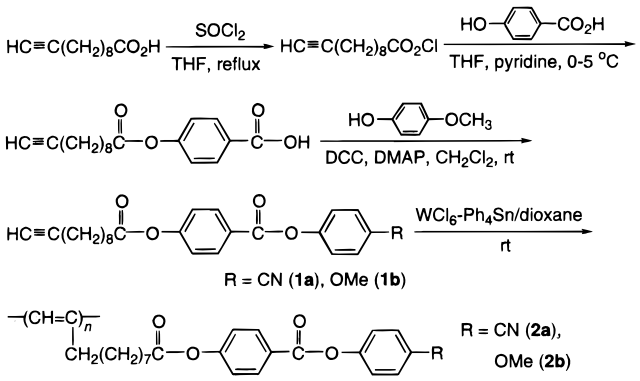


polymer chains may be aligned by mechanical forces to macroscopically ordered structures, and thus, the SCLCPs with rigid backbones may show intriguing mesomorphic properties. With this in mind, in this study, we synthesized two SCLCPs that possess the rigid polyacetylene backbones (**2**; Scheme 1) and investigated their responses to the applied external mechanical forces. We here demonstrate that the rigid backbone in a properly designed SCLCP system can play an active role in promoting and maintaining the molecular orientations induced by the simple mechanical perturbations. Thus, the liquid crystalline polyacetylene with the methoxy tails (**2b**) exhibits rotation-induced high-strength disclinations, shear-induced inversion walls, and solidification-induced banded textures, which have rarely been observed in the conventional SCLCPs with flexible backbones.[6]

## Results and Discussion

**Monomer Synthesis and Crystal Polymorphism.** We synthesized the mesogen-containing acetylene monomers (**1**) by two consecutive esterification reactions, using 10-undecynoic acid as a starting material. As shown in Scheme 1, the alkynoic acid is treated with thionyl chloride, and the resulting acid chloride is allowed to react with 4-hydroxybenzoic acid in the presence of pyridine to complete the first esterification reaction.[7] The second esterification is realized by the direct reaction of 10-((4-carboxyphenoxy)carbonyl)-1-decyne with 4-cyanophenol or 4-methoxyphenol in the presence of 1,3-dicyclohexylcarbodiimide (DCC) and 4-(dimethylamino)pyridine (DMAP).[8] The final products (**1**) are isolated by silica gel column chromatography followed by recrystallization. The purified monomers are characterized by spectroscopic methods, and satisfactory analysis data are obtained (see Experimental Section).

The monomer with the cyano tail (**1a**) exhibits interesting thermal transition behavior. When the crystalline sample of **1a** is heated, it shows two endothermic peaks at 84.7 and 103.3 °C before melting into the isotropic state (Figure 1A). The transitions are enantiotropic, and two exothermic peaks are observed at 86.1 and 70.5 °C in the differential scanning calorimetry (DSC) thermogram when the sample is cooled.

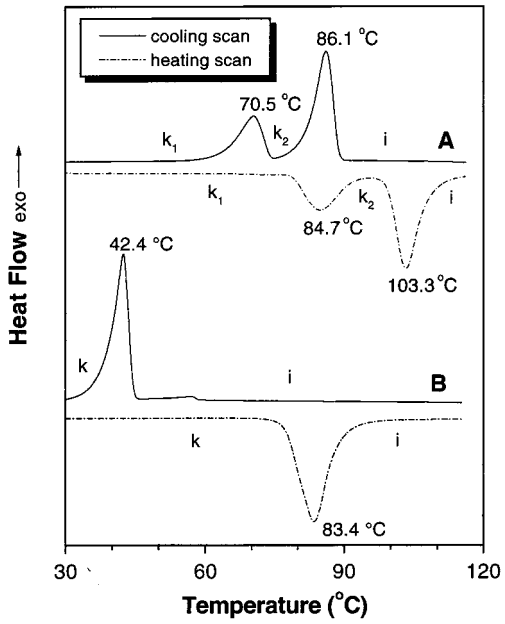


**Figure 1.** DSC thermograms of (A) **1a** and (B) **1b** measured under nitrogen at a scanning rate of 10 °C/min.

At first glance, the DSC curves look like typical liquid crystalline transition thermograms. We used a polarized optical microscope (POM) to investigate the thermal transition processes associated with the DSC peaks. The POM observations reveal that **1a** is not liquid crystalline. The peaks on the high-temperature side in Figure 1A are responsible for the melting and crystallization transitions, while those on the low-temperature side are associated with crystal−crystal (k−k) transitions in the solid state. Figure 2 shows two POM photographs taken at the different crystalline phases. When **1a** is cooled from its isotropic state, it *solidifies* and its crystalline phase at 93 °C displays lumberlike mosaic textures. The textures remain unchanged until the sample is cooled to 74 °C, at which the "lumbers" break. Such crystal polymorphism has been reported for sodium, ammonium, phosphonium, and pyridinium salts of amphiphilic molecules[9] but has seldom been observed in nonionic organic molecular crystal systems.

Because of the high acidity of the acetylenic protons, terminal alkynes are among the best-studied donors of C−H···X hydrogen bonds, where X is an atom of high electronegativity or a group rich in $\pi$-electrons.[10] The

(7) (a) Zhang, X.; Ozcayir, Y.; Feng, C.; Blumstein, A. *Polym. Prepr.* **1990**, *31* (1), 597. (b) Advincula, R. C.; Roberts, M. J.; Zhang, X.; Blumstein, A.; Duran, R. S. In *Macromolecular Assemblies in Polymeric Systems*; Stroeve, P., Balazs, A. C., Eds.; American Chemical Society: Washington, DC, 1992; Chapter 2, p 10.

(8) Furniss, B. S.; Hannaford, A. J.; Smith, P. G.; Tatchell, A. R. *Vogel's Textbook of Practical Organic Chemistry*, 5th ed.; Longman: Essex, U.K., 1989.

(9) (a) Ubbelohde, A. R.; Michels, H. J.; Duruz, J. J. *Nature* **1970**, *228*, 50. (b) Busico, V.; Corradini, P.; Vacatello, M. *J. Phys. Chem.* **1982**, *86*, 1033. (c) Sudholter, E. J. R.; Engberts, J. B. F.; de Jeu, W. H. *J. Phys. Chem.* **1982**, *86*, 1908. (d) Margomenou-Leonidopoulou, G. *Thermochim. Acta* **1988**, *134*, 49. (e) Bruce, D. W.; Estdale, S.; Guillon, D.; Heinrich, B. *Liq. Cryst.* **1995**, *19*, 301. (f) Bowlas, C. J.; Bruce, D. W.; Seddon, K. R. *Chem. Commun.* **1996**, 1625. (g) Kanazawa, A.; Tsutsumi, O.; Ikeda, T.; Nagase, Y. *J. Am. Chem. Soc.* **1997**, *119*, 7670.

(10) (a) Steiner, T.; Lutz, B.; van der Maas, J.; Schreurs, A. M. M.; Kroon, J.; Tamm, M. *Chem. Commun.* **1998**, 171. (b) Kariuki, B. M.; Harris, K. D.; Philp, D.; Robinson, J. M. A. *J. Am. Chem. Soc.* **1997**, *119*, 12679. (c) Gavezzotti, A.; Filippini, G.; Kroon, J.; van Eijck, B. P.; Klewinghaus, P. *Chem. Eur. J.* **1997**, *3*, 893. (d) Weiss, H.-C.; Boese, R.; Smith, H. L.; Haley, M. M. *Chem. Commun.* **1997**, 2403. (e) Desiraju, G. *Chem. Commun.* **1997**, 1475. (f) Steiner, T. *Chem. Commun.* **1997**, 727.

**Table 1. Phase Transitions and Corresponding Thermodynamic Parameters of the Alkyne Monomers and Polymers[a]**

| | | $T$, °C ($\Delta H$, kJ mol$^{-1}$; $\Delta S$, J mol$^{-1}$ K$^{-1}$) | |
|---|---|---|---|
| no. | sample | heating[b] | cooling[c] |
| | | Monomers | |
| 1 | **1a** | $k_1$ 84.7 (15.6; 43.6) $k_2$ 103.3 (32.3; 85.8) i | i 86.1 (−32.2; −89.5) $k_2$ 70.5 (−16.3; −47.4) $k_1$ |
| 2 | **1b** | k 83.4 (53.0; 148.7) i | i 42.4 (−43.8; −138.9) k |
| | | Polymers | |
| 3 | **2a** | g 80.4 (2.5; 7.1) $s_A$ 194.8 (0.8; 1.7) i | i 189.5 (−1.0; −2.1) $s_A$ 71.3 (−1.7; −5.0) g |
| 4 | **2b** | g 95.6 (2.6; 7.0) $s_A$ 113.9 (0.8; 2.0) n 140.8 (0.9; 2.1) i | i 132.5 (−1.0; −2.3) $s_A$ 104.3 (−0.9; −2.4) n 81.5 (−3.0; −8.6) g |

[a] Measured by DSC under nitrogen at a scanning rate of 10 °C/min. Abbreviations: k, crystalline state; g, glassy state; n, nematic phase; s, smectic phase; i, isotropic state. [b] Data taken from the 2nd heating scan. [c] Data taken from the 1st cooling scan.

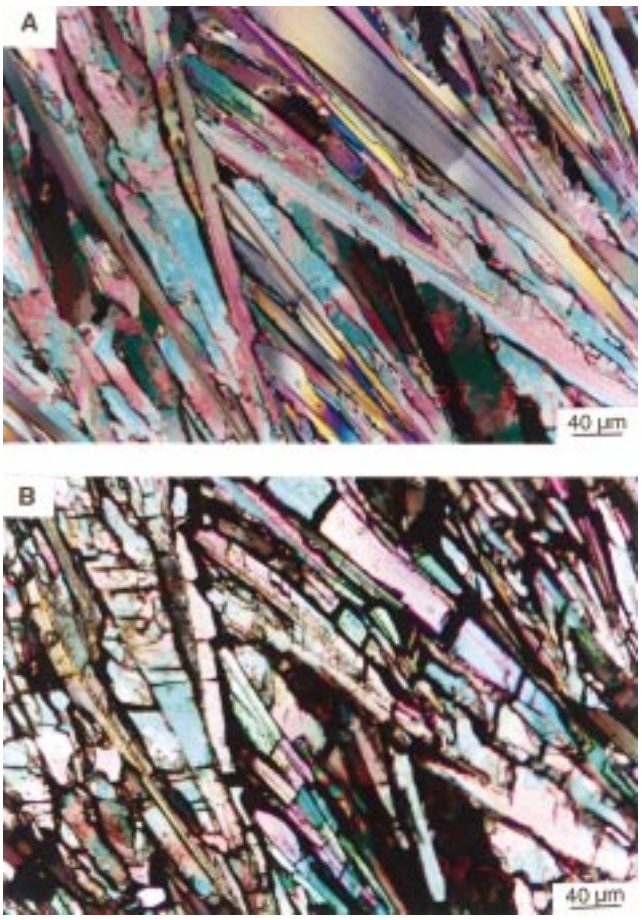


**Figure 2.** Polarized optical micrographs taken upon cooling **1a** from its isotropic state to (A) 93 °C and (B) 74 °C.

cyanoalkyne **1a** possesses an acetylene (≡C−H) donor and a cyano (N≡C−) acceptor. Intermolecular ≡C−H···N≡C− hydrogen bonds are thus likely to form, which may be responsible for the observed crystal polymorphism. When cooled from its isotropic state, the **1a** molecules may align in a head-to-tail fashion through the intermolecular hydrogen bonds, giving rise to the ordered $k_2$ structure. Further cooling may promote better ordering or crystallization of the polymethylenic (octyl) spacers, resulting in the formation of the $k_1$ phase. The volume shrinkage accompanying the $k_2$−$k_1$ transition in the solid state may account for the observed breakage of the lumberlike mosaic textures (cf. Figure 2B). Since the formation of the $k_2$ phase involves translational movements and hydrogen bonding, the enthalpy ($\Delta H$) and entropy changes ($\Delta S$) associated with the transition process would be larger than those for the $k_1$ phase formation, in which the further packing is realized only by localized translational movements of the molecules and conformational changes such as rotational motion of the alkyl spacers. This argument is supported by the $\Delta H$ and $\Delta S$ data calculated from the DSC thermograms. The $|\Delta H|$ and $|\Delta S|$ values for the i−$k_2$ transition are about two times higher than those for the $k_2$−$k_1$ transition during the cooling scan, while the $\Delta H$ and $\Delta S$ for the $k_1$−$k_2$ transition are about two times lower than those for the $k_2$−i transition during the heating scan (Table 1, no. 1).

The POM observations also reveal the involvement of transient liquid droplets in the $k_1$−$k_2$ transition during the heating scan. Thus the crystal polymorphism may also be understood in following way: When **1a** is warmed, the thermal agitation perturbs the packing of the octyl spacers first at a relatively low temperature (84.7 °C) because a relatively small amount of energy is needed for the so-called "conformational melting" transition.[9] Further heating then breaks all the ordered structures held by the intermolecular hydrogen bonds, thus rendering the whole system completely isotropic.

The monomer with the methoxy tail (**1b**) is not liquid crystalline either. It, however, displays only one set of enantiotropic transition peaks during the heating and cooling scans (Figure 1B). In other words, different from its **1a** cousin, **1b** does not show the crystal polymorphism, probably due to the lack of the hydrogen bonding. During the heating scan, only one transition peak is observed at 83.4 °C, whereas the peak at the higher temperature responsible for the breakage of the hydrogen bonds is not detected. A supercooling of >40 °C is needed to realize the crystallization transition during the cooling scan, providing circumstantial evidence for the weak interaction between the **1b** molecules.

We are able to confirm the intermolecular ≡C−H···N≡C− hydrogen bonds in **1a** by X-ray crystallography,[11] but have had difficulty in growing high-quality single crystals of **1b** for reliable structural determination. The IR analysis, however, gives some clue to the molecular interaction in **1b**. The acetylenic C−H stretching band of **1a** is located at 3260 cm$^{-1}$ (Figure 3A), which is 26 cm$^{-1}$ lower than that of **1b** (3286 cm$^{-1}$; Figure 4A). The red-shift of 26 cm$^{-1}$ in $\nu_{\equiv C-H}$ of **1a** is the consequence of the hydrogen bonding, because the ≡C−H···N≡C− interaction weakens the C−H bond, thus moving the

(11) H···N bond: 2.424 Å. C−H···N angle: 172.8°. The hydrogen bond in **1a** is shorter in length and more straight in geometry than that (2.530 Å; 154.3°) in 10-{[(4′-cyano-4-biphenylyl)oxy]carbonyl}-1-decyne [or HC≡C$(CH_2)_8CO_2$-biph-C≡N], the cyanoalkyne containing the biphenyl (biph) mesogen prepared in our previous work.[12] The H···N distance is similar to the H···O distance (typical value: 2.1−2.6 Å) for the ≡C−H···O hydrogen bonds.[10] Details of the single-crystal structure determination by the X-ray analysis of **1a** will be published by X. Kong, I. Williams, and B. Z. Tang in a separate paper.

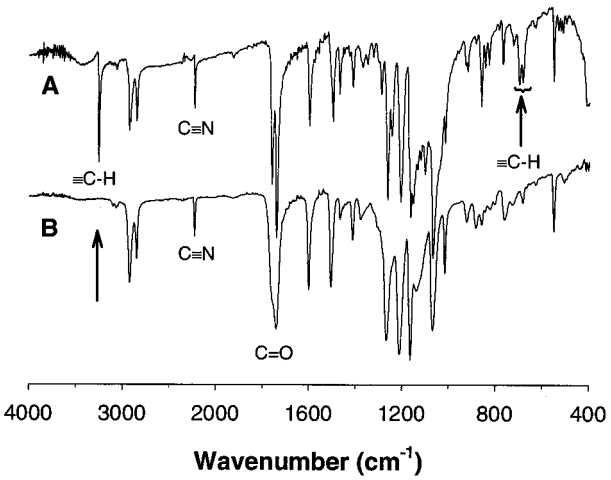


**Figure 3.** IR spectra of (A) **1a** and (B) **2a**.

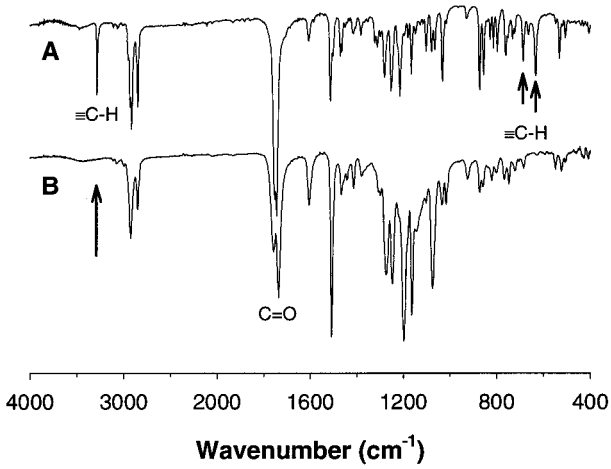


**Figure 4.** IR spectra of (A) **1b** and (B) **2b**.

C−H vibration to the lower frequency.[10,15] In other words, owing to the weak intermolecular interaction in **1b**, the C−H stretching occurs at the relatively high frequency.

**Polymer Synthesis and Structural Characterization.** Quite often, a nonliquid-crystalline calamitic monomer becomes mesomorphic after polymerization due to the "polymer effects".[5,6,12] We thus tried to polymerize **1** in the hope that the polymerization will stabilize the packing of the mesogenic groups. The polar cyano functional group is known to be "toxic" to the classical metathesis catalysts for acetylene polymerizations in toluene,[13,14] but in our previous work, we found that the $WCl_6$−$Ph_4Sn$/dioxane complex was tolerant of the cyano functionality.[12] We thus employed the $WCl_6$−$Ph_4Sn$/dioxane complex to polymerize **1**. Stirring a dioxane solution of **1a** under nitrogen in the presence of $WCl_6$ and $Ph_4Sn$ for 24 h gives a yellow powdery product, which is isolated in 46.8% yield by repeated precipitation of its dioxane solutions into methanol and then ether. Gel permeation chromatography (GPC) analysis of the product gives a polystyrene-calibrated $M_w$ of 29 000 and a polydispersity ($M_w/M_n$) of 1.7, confirming the polymeric nature of the product. Similarly, **1b** is polymerized by the $WCl_6$−$Ph_4Sn$/dioxane complex to a yellow powdery product in 35.3% yield, whose $M_w$ and $M_w/M_n$ are estimated by GPC to be 28 400 and 2.7, respectively. Thus, although the polymer yields are only moderate, the results prove that the $WCl_6$−$Ph_4Sn$/dioxane complex is also tolerant to the ester and methoxy functionalities.

The molecular structures of the polymeric products are characterized by spectroscopic methods. Figure 3 compares the IR spectra of **1a** and its polymer. As discussed above, the monomer absorbs at 3260 $cm^{-1}$ due to the acetylenic C−H stretching vibration. The in-plane and out-of-plane ≡C−H bending vibrations occur respectively at 698 and 684 $cm^{-1}$. All the acetylenic absorption bands disappear in the spectrum of the polymer, confirming that the polymerization is realized by the reaction of the acetylene triple bond. The absorption bands of the cyano and ester groups still remain; that is, the polar function groups survive the acetylene polymerization reaction. Similar results are obtained from the comparison of the IR spectra of **1b** and its polymer (Figure 4): The polymer does not show the acetylenic absorption bands, while the ester functionality survives the polymerization reaction.

Figure 5 shows the $^1H$ NMR spectra of **1a** and its polymer. The spectrum of the monomer is measured in chloroform while that of the polymer is measured in THF. The polymer is only partially soluble in chloroform, probably due to the strong interchain interaction in the polymer system. The acetylene proton of **1a** absorbs at $\delta$ 1.95, which disappears in the spectrum of its polymer. A new peak appears at around $\delta$ 6.1, which is assignable to the absorption by the cis olefin proton in the polymer main chain.[12,16,17] The peak is weak, because another part of the olefin protons, i.e., the trans proton, absorbs downfield in the aromatic region. The peak is quite broad, probably due to the inhomogeneous distribution of the stereosegments. Another possible cause for the peak broadening is the unpaired electrons or solitons, whose existence has been detected by electron spin resonance (ESR) in many (substituted) polyacetylenes.[4,14] The unpaired electron in the polyacetylene main chain may abstract a hydrogen from the neighboring methylene group, resulting in the formation of a side-chain allylic radical. The absorption peak of the allylic proton in the polyalkyne thus should be weak and broad, which is indeed the case, as shown in Figure

(12) (a) Tang, B. Z.; Kong, X.; Wan, X.; Peng, H.; Lam, W. Y.; Feng, X.-D.; Kwok, H. S. *Macromolecules* **1998**, *31*, 2419. (b) Kong, X.; Wan, X.; Kwok, H. S.; Feng, X.-D.; Tang, B. Z. *Chin. J. Polym. Sci.* **1998**, *16*, 185.

(13) (a) Ho, T. H.; Katz, T. J. *J. Mol. Catal.* **1985**, *28*, 359. (b) Carlini, C.; Chien, J. C. W. *J. Polym. Sci. Polym. Chem. Ed.* **1984**, *22*, 2749. (c) Deits, W.; Cukor, P.; Rubner, M.; Jopson, H. *Ind. Eng. Chem. Prod. Res. Dev.* **1981**, *20*, 696. (d) Hankin, A. G.; North, A. M. *Trans. Faraday Soc.* **1967**, *63*, 1525. (e) MacNulty, B. J. *Polymer* **1967**, *63*, 1525. (f) Mison, A.; Noughchi, H.; Noda, S. *J. Polym. Sci. Polym. Lett. Ed.* **1966**, *4*, 985.

(14) (a) Masuda, T.; Higashimura, T. *Adv. Polym. Sci.* **1987**, *81*, 121. (b) Schrock, R. R. *Acc. Chem. Res.* **1990**, *23*, 158. (c) Ginsburg, E. J.; Gorman, C. B.; Grubbs, R. H. In *Modern Acetylene Chemistry*; Stang, P. J., Diederich, F., Eds.; VCH: New York, 1995; p 353.

(15) (a) Lin-Vien, D.; Colthup, N. B.; Fateley, W. G.; Grasselli, J. G. *The Handbook of Infrared and Raman Characteristic Frequencies of Organic Molecules*; Academic Press: Boston, MA, 1991. (b) Roeges, N. P. G. *A Guide to the Complete Interpretation of Infrared Spectra of Organic Structures*; Wiley: New York, 1994.

(16) (a) Tang, B. Z.; Kong, X.; Wan, X.; Feng, X.-D. *Macromolecules* **1997**, *30*, 5620. (b) Tang, B. Z.; Poon, W. H.; Leung, S. M.; Leung, W. H.; Peng, H. *Macromolecules* **1997**, *30*, 2209.

(17) (a) Simionescu, C. I.; Percec, V. *J. Polym. Sci., Polym. Symp.* **1980**, *67*, 43. (b) Simionescu, C. I.; Percec, V.; Dumitrescu, S. *J. Polym. Sci., Polym. Chem. Ed.* **1977**, *15*, 2497.

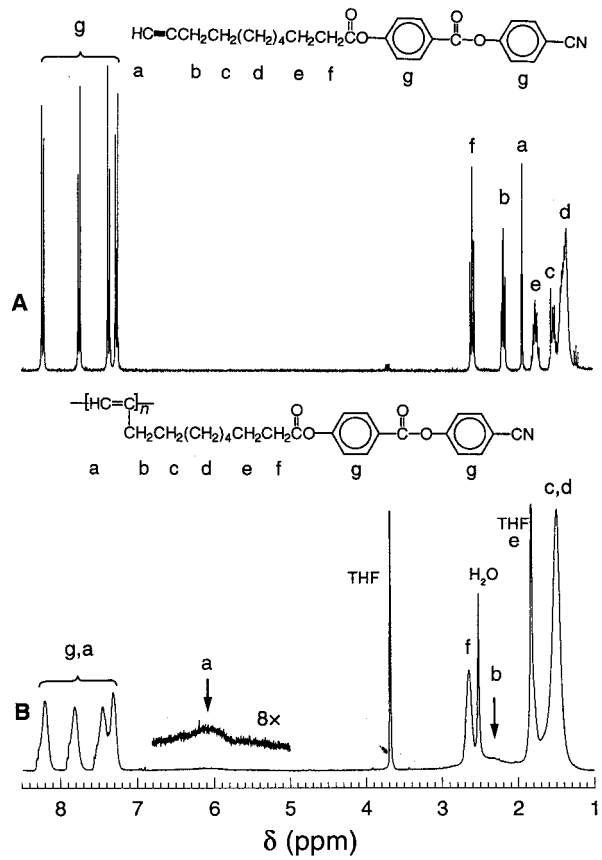


**Figure 5.** $^1$H NMR spectra of (A) **1a** in chloroform-*d* and (B) **2a** in THF-$d_8$.

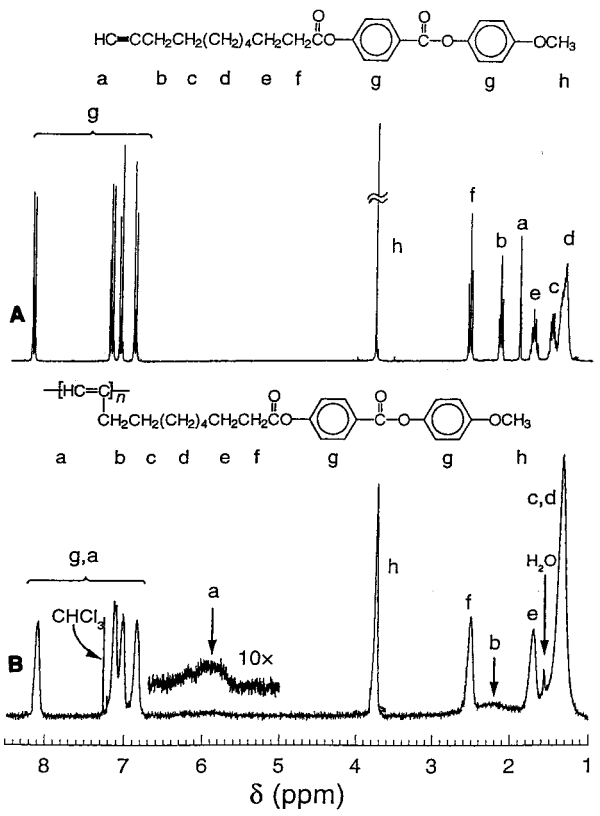


**Figure 6.** $^1$H NMR spectra of (A) **1b** and (B) **2b** in chloroform-*d*.

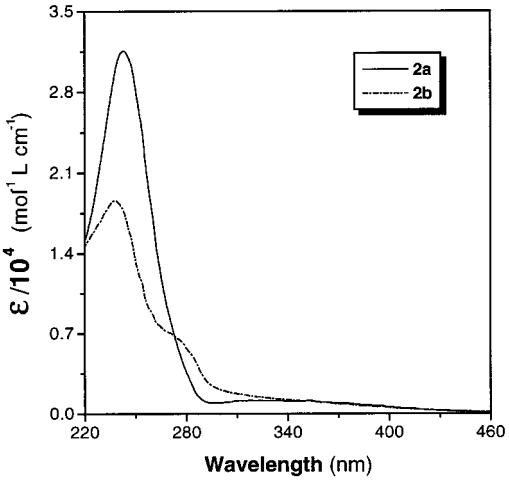


**Figure 7.** UV spectra of **2a**,**b** in THF.

5B (signal "b"). No unexpected signals are observed, and all the peaks are assignable to the absorption by the appropriate protons as marked in Figure 5B. The NMR spectral data thus confirm that the acetylene polymerization has taken place and that the molecular structure of the polymeric product is indeed **2a**, as shown in Scheme 1. Similarly, the molecular structure of the polymer obtained from **1b** is confirmed to be **2b** by the NMR analysis (Figure 6). It is worth mentioning that the NMR spectrum of **2b** is measured in deuterated chloroform because of its excellent solubility in the common NMR solvent (vide infra).

The UV spectra of **2** are shown in Figure 7. While neither **1a** nor **1b** absorbs above 300 nm, the electronic transition spectra of both **2a** and **2b** extend well into the visible region, due to the absorption of the polyacetylene backbone consisting of the alternating double bonds. Interestingly, in the spectral region below 300 nm, **2a** shows only one absorption peak at 243 nm whereas **2b** exhibits two peaks at 237 and 276 nm, suggesting that the two benzene rings in the mesogenic pendants of **2a** are in a similar electronic environment but those of **2b** possess different transition energies.

**Mesomorphic Properties.** To investigate the mesomorphic properties of the polymers, we first checked their thermal stability. Poly(1-alkynes) such as poly(1-butyne) $\{-[CH{=}C(CH_2CH_3)]_n-\}$[18] and poly(1-hexyne) $\{-[CH{=}C(CH_2CH_2CH_2CH_3)]_n-\}$,[19] which may be considered as the parent forms of **2**, are thermally unstable and readily lose their weights at temperatures as low as ca. 150 °C. Neither **2a** nor **2b**, however, loses any weight below 300 °C in the thermogravimetric analysis (TGA; Figure 8). That is, they are thermally much more stable than the corresponding poly(1-alkynes) without the mesogenic moieties. The high thermal stability of **2** may stem from the "jacket effect".[12,16,20] The thermally stable mesogenic pendants may form a protective jacket surrounding the polyacetylene main chain, shielding the polymer backbone from the thermal attack.

As discussed above, the monomers are nonmesomorphic. To check whether the polymers are liquid crystal-

(18) Masuda, T.; Okano, Y.; Tamura, K.; Higashimura, T. *Polymer* **1985**, *26*, 793.

(19) Masuda, T.; Tang, B. Z.; Higashimura, T.; Yamaoka, H. *Macromolecules* **1985**, *18*, 2369.

(20) Tang, B. Z.; Wan, X.; Kwok, H. S. *Eur. Polym. J.* **1998**, *34*, 341.

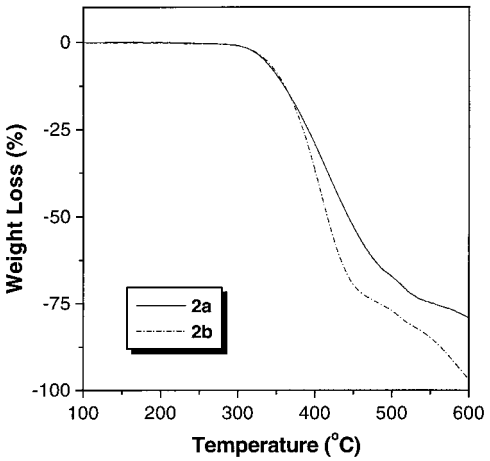


**Figure 8.** TGA thermograms of **2a**,**b** measured under nitrogen at a heating rate of 20 °C/min.

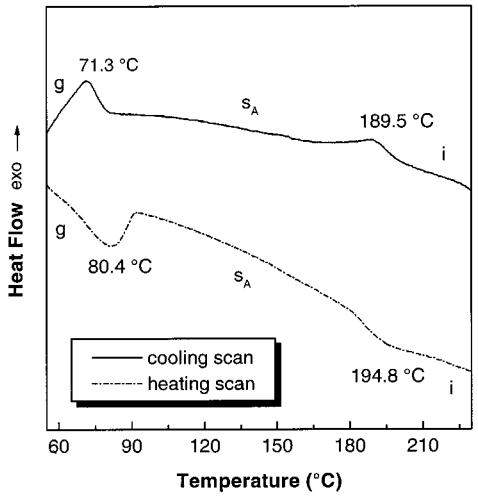


**Figure 9.** DSC thermograms of **2a** measured under nitrogen at a scanning rate of 10 °C/min.

line, we investigated their thermal transition processes by DSC. Figure 9 shows the DSC thermograms of **2a**. The polymer enters the smectic A mesophase at 80.4 °C during the second heating scan. The mesophase is stable in a temperature range over 100 °C before **2a** finally melts to isotropic liquid at 194.8 °C. It thus becomes clear that the polymerization has stabilized the ordering of the mesogenic groups. No other unexpected signals are observed in the DSC thermogram except the peaks associated with the melting and isotropization transitions, thus once again proving the thermal stability of the polymer.

The thermal transitions are enantiotropic, and the polymer shows two peaks at 189.5 and 71.3 °C associated respectively with the i−$s_A$ and $s_A$−k transitions during the cooling scan. The difference between the isotropization temperatures ($T_i$) of the polymer detected by DSC during the heating and cooling scans is quite small ($\Delta T_i = 5.3$ °C), compared to that (17.2 °C) of the monomer (cf. Figure 1A and Table 1, no. 1). The conformation of the rigid polyacetylene main chains may have not been completely randomized by the thermal agitation, and thus the ordering of the mesogenic pendants can be realized by a small extent of supercooling. Such ordering transition would involve a small entropy change, which is indeed the case, as shown in Table 1 (no. 3; $\Delta S_{i-s} = -2.1$ J mol$^{-1}$ K$^{-1}$).

The polymer exhibits typical $s_A$ textures in the mesomorphic temperature range. Figure 10 shows the dynamic process of the formation of the focal-conic fan texture. When **2a** is cooled from the isotropic state to 185 °C, many small bâtonnets emerge from the homeotropic dark background. The bâtonnets grow to bigger domains when the sample is further cooled, and interestingly, parallel bands form in the direction normal to the long axes of the domains (Figure 10B). When the temperature further drops, the domain further grows but the in-domain banded structure persists until the perfect focal-conic textures finally form (Figure 10D). Such transient banded textures have also been observed in the dynamic processes of the $s_A$ phase formation of other polyacetylenes such as −{CH=C[$(CH_2)_8CO_2$-biph-CN]}$_n$−[12] and −$(CH{=}CR)_n$−[21] [R = $(CH_2)_2CO_2(CH_2)_6$-OCO-biph-$OC_9H_{19}$, $(CH_2)_3CO_2$-biph-$OC_7H_{15}$, $(CH_2)_m$-OCO-biph-$OCOC_{11}H_{23}$ ($m$ = 3, 4), $(CH_2)_mO(CH_2)_6O$-biph-$OC_6H_{13}$ ($m$ = 3, 8), $(CH_2)_m$OCO-biph-$OC_7H_{15}$ ($m$ = 4, 9)], suggesting that the in-domain band formation is a common phenomenon observable in the smectic polyacetylene systems.

Using the quenching technique developed in our previous work,[12] we measured the X-ray diffraction (XRD) data of **2a** rapidly quenched by liquid nitrogen from its liquid crystalline state (165 °C). The diffractogram shows a sharp reflection at a low angle of $2\theta$ = 3.32° (Figure 12), from which, a $d$-spacing of 26.6 Å is derived by Bragg's law ($2d \sin\theta = n\lambda$). The existence of the sharp maximum is indicative of some type of long-range positional order, which takes the mesophase out of nematic classification.[22] The calculated molecular length ($l$) for the repeat unit of **2a** at its most extended conformation is 26.7 Å, which is identical to the experimentally obtained layer thickness (26.6 Å) within experimental error, thus confirming the $s_A$ nature of the mesophase. The peak centered at $2\theta$ = 20.31° ($d$ = 4.4 Å) corresponds to the spacing of the polymethylenic (octyl) spacers.[23] In our previous study, the poly(cyanoalkynes) containing the biphenyl mesogens showed diffuse halos in the high-angle region.[12] The peak observed here is narrower and more intense, suggesting that the alkyl spacers in **2a** are better ordered. The small reflection in the mid-angle region ($2\theta$ = 5.57°) may be associated with the ordering of the mesogenic units with locally perturbed octyl spacers.[12]

The thermal transition processes of **2b** are more complex. The polymer shows enantiotropic smectic A and nematic mesophases in the temperature region of 80−140 °C during the heating and cooling scans (Figure 12). The monomer needs a large extent of supercooling ($\Delta T_i$ = 41 °C) to realize the crystallization process (cf.

(21) (a) Lam, W. Y.; Lee, P. S.; Cheuk, K. L.; Tang, B. Z. *5th Symp. Chem. Res. HK* **1998**, O-44. (b) Lam. W. Y.; Lee, P. S.; Tang, B. Z. *Symp. Frontiers Chem*. **1997**, 465. (c) Lam, W. Y.; Wan, X.; Kong, X.; Tang, B. Z. *4th Symp. Chem. Res. HK* **1997**, 0−29.

(22) (a) Mariani, P.; Rustichelli, F.; Torquati, G. In *Physics of Liquid Crystalline Materials*; Khoo, I.-C., Simoni, F., Eds.; Gordon & Breach Science: New York, 1991; Chapter 1. (b) *Liquid Crystalline Order in Polymers*; Blumstein, A., Hsu, E. C., Eds.; Academic Press: New York, 1978. (c) *Liquid Crystalline and Mesomorphic Polymers*; Shibaev, V., Lam, L., Eds.; Springer-Verlag: New York, 1994.

(23) Kato, T.; Kubota, Y.; Uryu, T.; Ujiie, S. *Angew. Chem., Int. Ed. Engl.* **1997**, *36*, 1617.

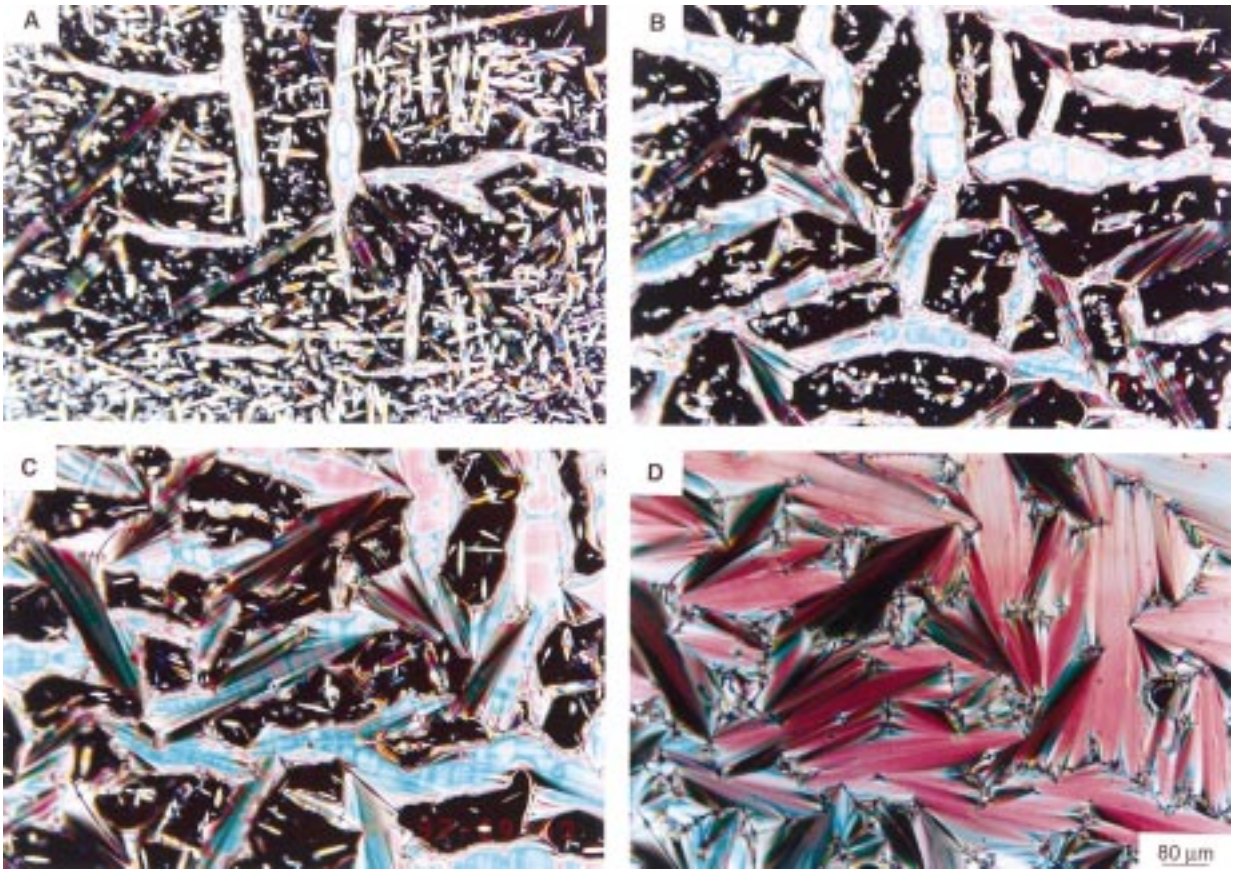


**Figure 10.** Textures observed on cooling **2a** from its isotropic state at a rate of 5 °C/min. Microphotographs were taken after annealing (A) at 185 °C for 5 min, (B) at 180 °C for 5 min, (C) at 175 °C for 5 min, and (D) at 160 °C for 48 min.

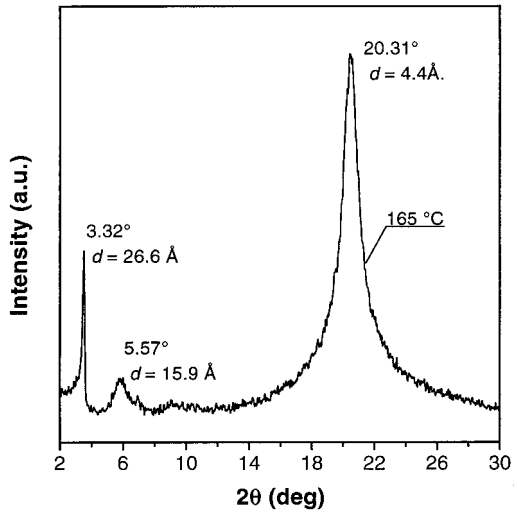


**Figure 11.** XRD patterns of **2a** quenched from its liquid crystalline state by liquid nitrogen.

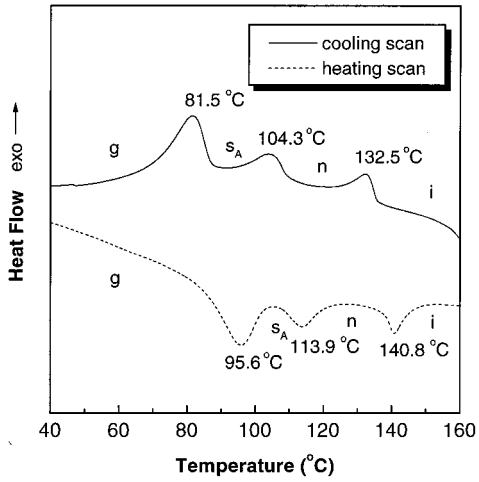


**Figure 12.** DSC thermograms of **2b** measured under nitrogen at a scanning rate of 10 °C/min.

Figure 1B and Table 1, no. 2), but the $\Delta T_i$ for the polymer is merely 8.3 °C, suggesting that the thermal perturbation has not completely messed up the packing of the rigid polyacetylene chains.

Figure 13 shows the POM photographs of **2b** taken at different mesophasic temperatures. The polymer displays schlieren textures with droplets when cooled from the isotropic state. The droplets are characteristic of nematic mesophase because they occur nowhere else.[24] There are many point singularities with two dark brushes in the schlieren textures, which further confirm the nematic nature of the mesophase because such singularity is not compatible with the smectic C structure.[24] Upon further cooling, coarse textures of disclination loops form (Figure 13B). Parallel stripes normal to the long axes of the loops develop when the temperature further drops. The stripes can be easily erased by heating and regenerated by cooling. Such striped loops have been observed by Hudson et al.[25] and Cladis and Torza[26] during the processes of nematic-to-

(24) (a) Demus, D.; Richter, L. *Textures of Liquid Crystals*; Verlag Chemie: Weinheim, Germany, 1978. (b) Gray, G. W.; Goodby, J. W. G. *Smectic Liquid Crystals: Textures and Structures*; Leonard Hill: London, 1984. (c) Zhou, Q. F.; Wang X. J. *Liquid Crystalline Polymers*; Science Press: Beijing, 1994.

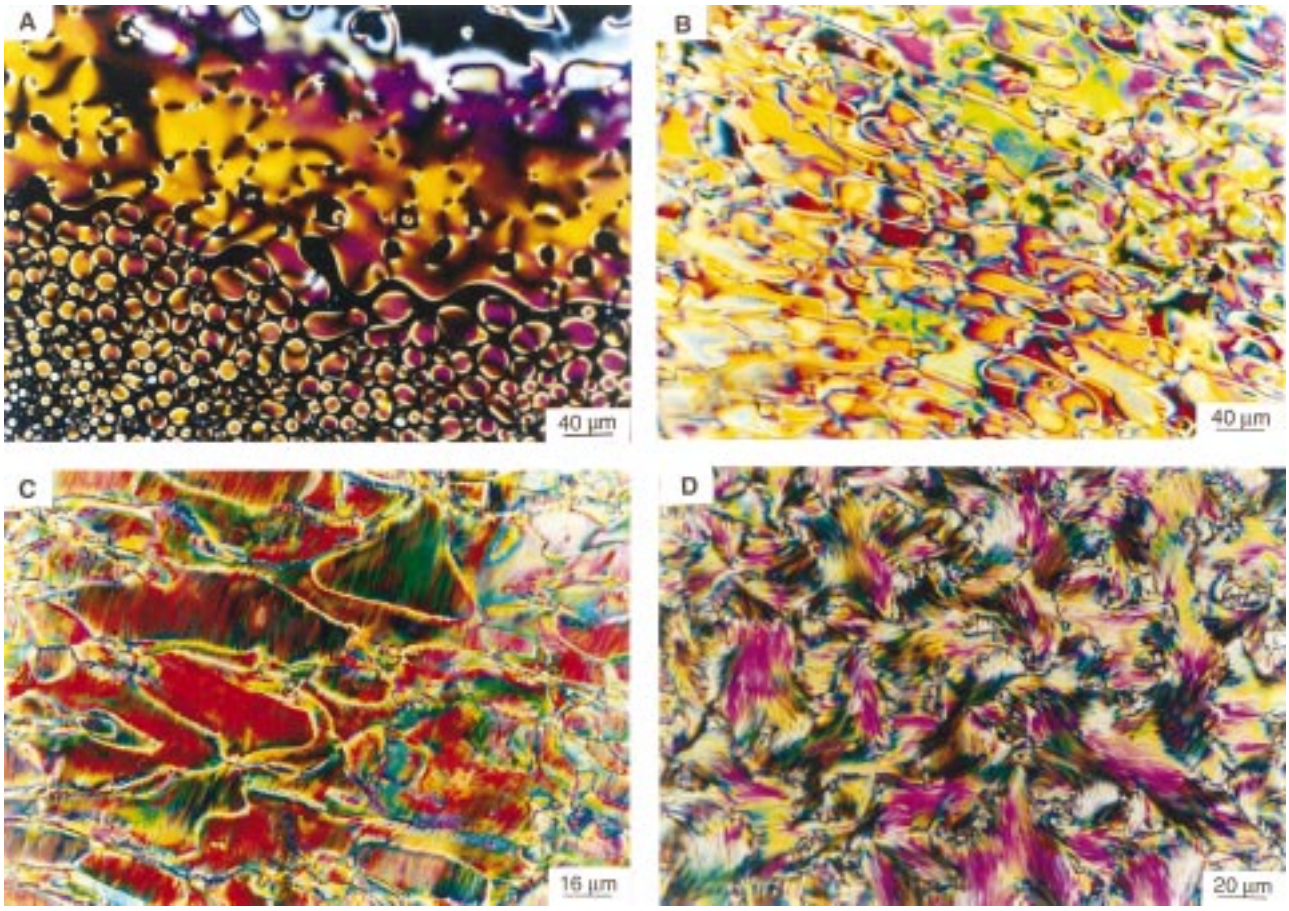


**Figure 13.** Textures observed on cooling **2b** from its isotropic state at a rate of 5 °C/min. Microphotographs were taken after annealing for 2 min at (A) 139.5, (B) 131.0, (C) 110.0, and (D) 100.0 °C.

smectic transitions. The striped loops evolve to striated feather textures when **2b** is cooled to 100 °C (Figure 13D).

The smectic **2b** rapidly quenched by liquid nitrogen from 100 °C displays a sharp Bragg reflection at a low angle of $2\theta = 3.41°$, a large peak at a high angle of $2\theta = 20.37°$, and small bumps in the mid-angle region (Figure 14). The layer thickness derived from the Bragg angle of $2\theta = 3.41°$ is 25.9 Å, which is somewhat shorter than the calculated molecular length ($l = 26.9$ Å). Such discrepancy (within 5%) is quite common, due to the molecular orientational disorder and the aliphatic chain random motion.[6,27] Nevertheless, the XRD data confirm the $s_A$ nature of the mesophase at 100 °C,[22] although the POM texture is atypical of the $s_A$ mesophase (cf. Figure 13D).

According to the literature, the typical XRD pattern of a nematic liquid crystal is characterized by (i) a diffuse peak in the high-angle region and (ii) a broad peak (rarely visible due to its low intensity) in the low-angle region.[22a] The XRD diagram of **2b** quenched from

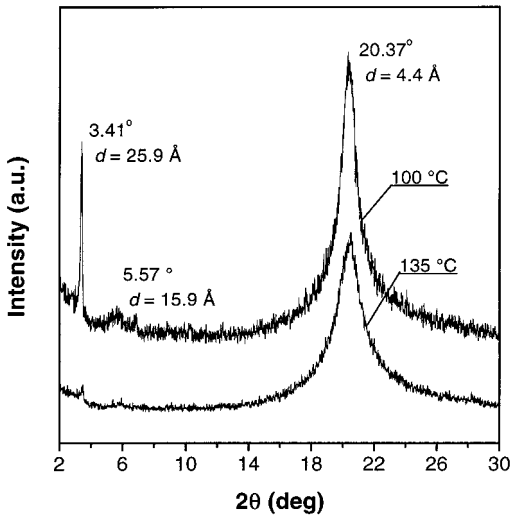


**Figure 14.** XRD patterns of **2b** quenched from its liquid crystalline states by liquid nitrogen.

135 °C actually has the two features: it shows a diffuse halo at $2\theta = 20.37°$ and a barely recognizable small hump at $2\theta = 3.41°$, thus verifying the nematicity of the mesophase at the high temperature.

**Mechanical Force Induced Molecular Alignments.** It is of both academic interest and practical significance to modulate the molecular alignments of liquid crystalline polymers by external forces. The macroscopic polymer processing techniques commonly utilize mechanical forces such as shear. The difference

(25) Hudson, S. D.; Lovinger, A. J.; Larson, R. G.; Davis, D. D.; Garay, R. O.; Fujishiro, K. *Macromolecules* **1993**, *26*, 5643.
(26) Cladis, P. E.; Torza, S. *J. Appl. Phys.* **1975**, *46*, 584.
(27) (a) *Liquid Crystalline Polymer Systems: Technological Advances*; Isayev, A. I., Kyu, T., Cheng, S. Z. D., Eds.; American Chemical Society: Washinton, DC, 1996. (b) *Liquid Crystal Polymers: from Structures to Applications*; Collyer, A. A., Ed.; Elsevier Applied Science: London, 1992. (c) *Liquid Crystallinity in Polymers: Principles and Fundamental Properties*; Ciferri, A., Ed.; VCH Publishers: New York, 1991. (d) *Liquid-Crystalline Polymers*; Weiss, R. A., Ober, C. K., Eds.; American Chemical Society: Washington, DC, 1990. (e) *Polymeric Liquid Crystals*; Blumstein, A., Ed.; Plenum Press: New York, 1985.

between **2** and conventional vinyl-polymer-type SCLCPs is the rigidity of the polymer backbones. The rigid polyacetylene backbone[28] possesses quite a long relaxation time; for example, the chain conformation frozen by the solvent evaporation during the preparation of poly[1-(trimethylsilyl)-1-propyne] films needs more than 2 weeks to relax back to the most probable conformation.[28a] A mechanically agitated polyacetylene system with proper viscosity may not quickly return back to the preperturbation state, thus offering the opportunity to generate macroscopic sample anisotropy by the application of mechanical forces.

In our previous work, we generated banded textures by shearing a poly(cyanoalkyne) containing the biphenyl mesogen, $-\{CH{=}C[(CH_2)_8CO_2\text{-biph-}CN]\}_n-$, in its liquid crystalline state.[12] We thus applied a shear force to the smectic **2a**, which also possesses the cyano tails, but unfortunately we failed to generate any banded textures. The polymer in the previous work is completely soluble in chloroform, a solvent of relatively low polarity.[29,30] The complete dissolution of **2a**, however, cannot be accomplished in chloroform but needs more polar solvents such as THF and dioxane[29,30] to be realized. The strong intermolecular interaction in **2a** may make the $s_A$ phase too viscous, which in turn makes it difficult for the polymer chains and mesogenic pendants to move and align along the shear direction.

The excellent solubility of **2b** in chloroform implies that the intermolecular interaction in **2b** is weaker than that in **2a**. The nematicity indicates that the lateral interaction of the mesogenic groups in **2b** is also weak. The weakly interacted side chains thus may serve as "internal plasticizers", helping the rigid polyacetylene main chains move in response to the applied external forces. To explore the possibility, we applied a rotational force to a nematic **2b** by circularly rotating the cover slide of the sample cell. After a few minutes, we observed the unusual schlieren textures (Figure 15): 2, 4, 6, and 8 extinction brushes emanating from the singularity cores, which correspond respectively to the disclination strengths ($s$) of $^1/_2$, 1, $^3/_2$, and 2. According to liquid crystal textbooks,[24] the experimentally "normally" observable disclinations are those with $s$ of $\pm^1/_2$ and $\pm1$. The disclinations with $|s| > 1$ have seldom been observed owing to the severe director field distortions involved.[6,31,32] The rotational agitation may have twisted the polyacetylene main chains and the long axes of the attached mesogenic pendants, thus generating the complex director fields. Owing to the long relaxation time of the rigid polyacetylene backbone, the twisted conformation cannot quickly relax back to the original "natural" state, thus enabling the observation of the high-strength disclinations. The observed singularity cores are relatively big in size. It is known that the energy of a disclination is in inverse proportion to the natural logarithm of its core radius,[31,32] and the strain energy thus may have forced the cores to grow in order to reduce the severity of the director field distortions at the singularities.

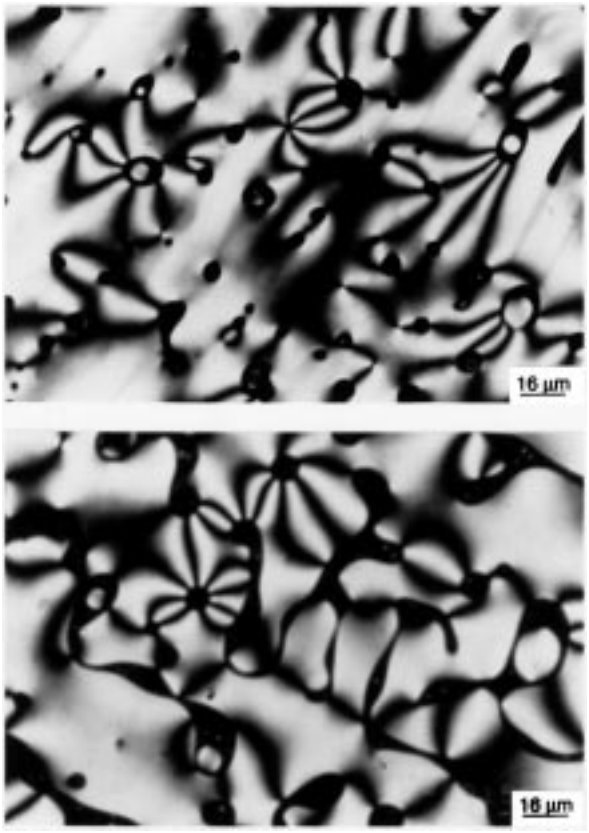


**Figure 15.** Schlieren textures with disclinations of strengths $^3/_2$ and 2, observed after a rotationally agitated **2b** is annealed at 136 °C for 3 (upper panel) and 5 min (lower panel).

Viney et al. observed the disclinations of strength $\pm^3/_2$ (also with relatively big singularity cores) in a circularly agitated nematic mesophase of a rigid small-molecular-mass compound, *p*-bis(4-biphenylethynyl)benzene ($C_6H_5C_6H_4C{\equiv}CC_6H_4C{\equiv}CC_6H_4C_6H_5$). The disclinations, however, were "transient" and extremely short-lived.[31b] The lifetime of the disclinations was so short (with the longest lifetime being shorter than 34 s) that even the photograph-taking of the textures was difficult to perform. The high-strength disclinations in our system, however, are much more stable. We also observed the mobility of the disclinations: Many of the microstructures shown in Figure 15 are obviously in the splitting transition processes from higher-strength disclinations to lower-strength ones, which are energetically more stable.[32] The motion, however, is in a much longer time scale compared to Viney's system, as evidenced by the little blurring of the microphotographs shown in Figure 15. The obvious difference between our and Viney's systems is the molecular weight (or viscosity). Thus, in addition to the long relaxation time, the high molecular weight of **2b** may have also contributed to the stabilization of the high-strength disclinations, in accordance with the theoretical prediction that the energy of a disclination is inversely proportional to the square root of molecular weight.[31,32] The nematic **2b** may

(28) (a) Masuda, T.; Iguchi, Y.; Tang, B. Z.; Higashimura, T. *Polymer* **1988**, *29*, 2041. (b) Masuda, T.; Higashimura, T. *Adv. Polym. Sci.* **1987**, *81*, 121. (c) Masuda, T.; Takashi, T.; Higashimura, T. *Macromolecules* **1985**, *18*, 311. (d) Hirao, T.; Teramoto, T.; Sato, T.; Norisuye, T.; Masuda, T.; Higashimura, T. *Polym. J.* **1991**, *23*, 925.

(29) Dipole moment: chloroform, 1.04 D (cf. THF, 1.75 D, and dioxane, 2.06 D); data taken from ref 30.

(30) *CRC Handbook of Chemistry and Physics*, 75th ed.; Lide, D. R., Ed.; CRC Press: Boca Raton, FL, 1994; p 9−42.

(31) (a) Nehring, J.; Saupe, A. *J. Chem. Soc., Faraday Trans. 2* **1972**, *68*, 1. (b) Viney, C.; Brown, D. J.; Dannels, C. M.; Twieg, R. J. *Liq. Cryst.* **1993**, *13*, 95.

(32) (a) Kleman, M. *Points, Lines and Walls*; Wiley: New York, 1983; Chapter 3. (b) Donald, A. M.; Windle, A. H. *Liquid Crystalline Polymers*; Cambridge University Press: Cambridge, U.K., 1992. (c) Qian, R.; Chen, S.; Song, W. *Macromol. Symp.* **1995**, *96*, 27.

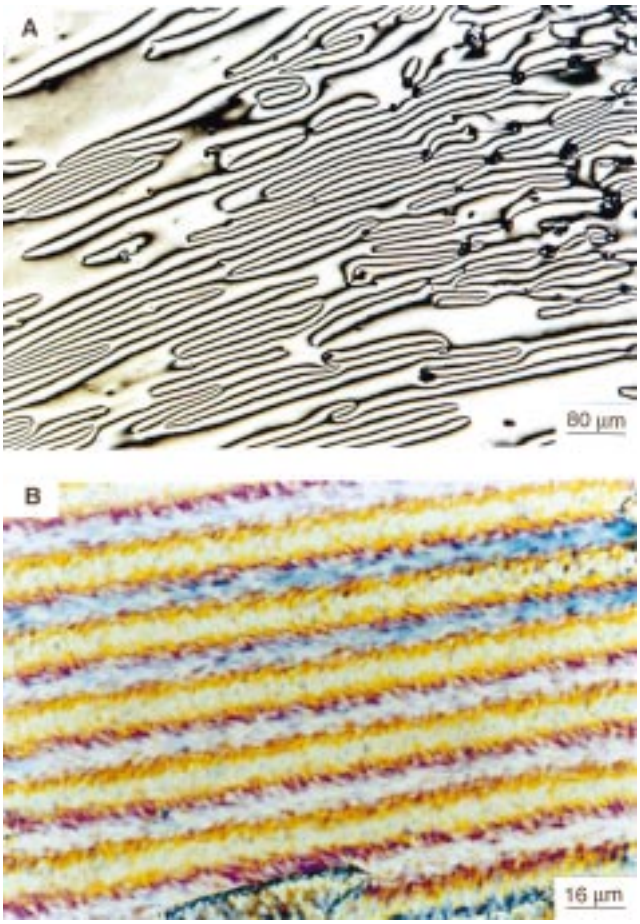


**Figure 16.** (A) Inversion walls observed after a sheared **2b** is annealed at 139.7 °C for 24 min and (B) banded textures observed after the inversion walls are naturally cooled to room temperature. The shear direction is parallel to the long axes of the walls and bands.

possess the just "right" viscosity, which is relatively "low" to allow the polyacetylene chains to respond to the vigorous external force in the dynamic state but is "high" enough to maintain the thus-generated complex director fields in the subsided state and to prevent the high-strength disclinations from rapid moving and annihilating.

The rotational force has helped generate the high-strength disclinations; what would happen if a translational force is applied to **2b**? Figure 16A shows the inversion walls observed after a nematic sample of **2b** is sheared at a temperature very close to its clearing point. Almost all of the inversion walls start and end at $\pm^1/_2$ singularities, with their long axes parallel to the direction of the shear force. The overall number of the disclinations in the sheared system is apparently smaller than that in the unsheared system (cf. Figure 13A). Since the disclinations are the discontinuity in the director orientation, the sheared system is thus better ordered. The shear force may have mobilized the disclinations by defining a direction in which they can move. Such movement would certainly annihilate some of the disclinations and increase the volume of the areas whose directors align parallel to the shear direction. The residual elastic defects may concentrate in the interfaces between the regions of uniform orientations, thus forming the inversion walls encircling the domains of high alignments.

At the molecular level, the uniform orientations may be achieved by the alignments of the polyacetylene chains and the mesogenic pendants along the shear direction. A forcibly aligned SCLCP with a flexible backbone by an external field may quickly "spring back" to its natural state via various relaxation processes[34] upon removal of the field, leading to the rapid loss of the orientations and the collapse of the inversion walls. The inversion walls in our system are stable long *after* the mechanical shearing at the nematic state. The long relaxation time of the rigid polyacetylene backbone thus may have played an important role in stabilizing the shear-induced orientations.

When the nematic **2b** is naturally cooled to room temperature, the solidification-induced ordering[35] further consumes more disclinations, giving rise to the well-ordered parallel bands (Figure 16B) with diameters of ca. 12 $\mu$m and lengths up to 1500 $\mu$m. Closer inspection of the banded textures reveals that the thicker bands are wrapped by helical threads. Such threads may be evolved from the stripes observed during the nematic−smectic transition (cf. Figure 13C). The transient stripes in the unsheared system develop into the randomly positioned striated-feather textures in the smectic mesophase. In the sheared system, however, the nematic−smectic transition would be accomplished by the alignments of the mesogenic pendants along the stretched polyacetylene main chains, thus giving rise to the threads ordered in the direction normal to the long axes of the thicker bands. The threads in the thinner walls separating the thicker bands are less ordered, probably due to the residue elastic distortion energy trapped in the defects.

The band formation is a ubiquitous phenomenon in the main-chain liquid crystalline polymer (MCLCP) systems but has seldom been observed in the conventional SCLCP systems.[36] The bands are aligned *perpendicular* to the shear direction in all the hitherto reported systems,[36b,37] but the bands in our system are aligned *parallel* to the shear direction. The solidification-induced band formation via the inversion walls is thus a new phenomenon and warrants further investigation. One intriguing possibility is that the bands are the "microtubes" consisting of bundles of stretched polyacetylene "nanowires" clad with the mesogenic jackets, as schematically illustrated in Chart 1. Such microtubes may exhibit anisotropic electrical conductivity and large optical nonlinearity, in addition to excellent thermal stability and high mechanical strength, and thus may find an array of potential applications as advanced materials in the high-technology industries.

(33) Ding, D.-K.; Thomas, E. L. *Macromolecules* **1993**, *26*, 6531. (b) Assender, H. E.; Windle, A. H. *Polymer* **1997**, *38*, 677.

(34) Moore, R. C.; Denn, M. M. In *High Modulus Polymers: Approaches to Design and Development*; Zachariades, A. E., Porter, R. S., Eds.; Marcel Dekker: New York, 1988.

(35) (a) Song, W.; Chen, S.; Jin, Y.; Qian, R. *Liq. Cryst.* **1995**, *19*, 549. (b) Hoff, M.; Keller, A.; Odell, J. A.; Percec, V. *Polymer* **1993**, *34*, 1800. (c) Chen, S.; Du, C.; Jin, Y.; Qian, R.; Zhou, Q. *Mol. Cryst. Liq. Cryst.* **1990**, *188*, 197.

(36) (a) Ge, J. J.; Zhang, A.; McCreight, K. W.; Ho, R.-M.; Wang, S.-Y.; Jin, X.; Harris, F. W.; Cheng, S. Z. D. *Macromolecules* **1997**, *30*, 6498. (b) Qian, R.; Chen, S. *Makromol. Chem., Makromol. Symp.* **1992**, *53*, 345.

(37) (a) *Rheology and Processing of Liquid Crystal Polymers*; Acierno, D., Collyer, A. A., Eds.; Chapman & Hall: London, 1996. (b) *Liquid Crystalline and Mesomorphic Polymers*; Shibaev, V., Lam, L., Eds.; Springer-Verlag: Hong Kong, 1994.

**Chart 1**

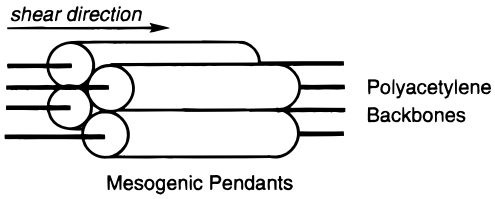


## Concluding Remarks

In summary, in this study, we designed and synthesized two mesogen-containing acetylene monomers (**1**). We observed the novel enantiotropic k−k transitions in the cyanoalkyne **1a** crystals, which represents a rare example of the crystal polymorphism in a nonionic molecular crystal system. The polymorphism is rationalized by the conformational packing of the long alkyl spacers and the hydrogen bonding between the acetylene head and the cyano tail. We polymerized both of the functional acetylene monomers using the $WCl_6$−$Ph_4$Sn/dioxane complex developed in our previous work,[12] which further expands the scope of the applicability and usefulness of the simple metal−halide catalyst system.

We observed the pronounced "tail effects" on the polymer properties: The polymer with the cyano tails (**2a**) is only partially soluble in chloroform and exhibits smecticity, while that with the methoxy tails (**2b**) is completely soluble in chloroform and exhibits nematicity in a moderate temperature region (95−140 °C). The highly polar cyano groups may have induced strong molecular interaction in **2a**,[38,39] but the weakly interacted methoxy-tailed side chains may have instead plasticized the rigid polyacetylene main chains.

We succeeded in modulating the molecular alignments of **2b** by mechanical perturbations. Thus, the rotational force generates the unusual high-strength disclinations, which have been reported for a couple of MCLCPs with rigid backbones,[40] but have never been observed in any conventional SCLCPs with flexible backbones. The translational shear creates the inversion walls, solidification of which produces the well-ordered parallel bands. The MCLCPs with rigid backbones often display the banded textures, but seldom do the SCLCPs with flexible backbones.[36] Thus, while structurally being a *S*CLCP, **2b** mesomorphically resembles a *M*CLCP in some aspects. Noting the unique feature in the molecular structure of **2b**, the rigid alternating-double-bond polyacetylene backbone may have played an important role in inducing the novel molecular alignments and hence the uncommon structure−property relationship.

The study on the SCLCPs with rigid backbones is a little explored research area, partly owing to the common belief that the rigid backbones interfere the packing of the mesogenic pendants and disturb the growth of the ordered domains. Our work presented here thus may trigger intensive molecular-engineering efforts in designing rigid-backbone SCLCPs and help develop a class of new liquid crystalline polymers with the combined advantages of a SCLCP (e.g., excellent tractability) and a MCLCP (e.g., superb orientability). Noting that many conjugated polymers are electrically conductive, optically nonlinear, and photo- and electroluminescent,[4,41] the development of the SCLCPs with the rigid conjugated backbones should contribute to the search for advanced materials with intriguingly novel electronic and optical properties.

## Experimental Section

**Materials.** Dioxane and THF were purchased from Aldrich, dried over 4 Å molecular sieves, and distilled from sodium benzophenone ketyl immediately prior to use. Thionyl chloride, pyridine, and 10-undecynoic acid were obtained respectively from Rediel de Haën, Nacalai Tesque, and Farchan Laboratory. Methylene chloride was purchased from Lab-Scan and was distilled over calcium hydride before use. 4-Hydroxybenzonic acid, 4-cyanophenol, 4-methoxyphenol, DCC, DMAP, tungsten(VI) chloride, tetraphenyltin, chloroform-*d*, and THF-$d_8$ were all purchased from Aldrich and used as received without further purification.

**Instrumentation.** The infrared spectra were recorded on a Perkin-Elmer 16 PC FT-IR spectrophotometer. The $^1$H and $^{13}$C NMR spectra were measured on a Bruker ARX 300 NMR spectrometer using chloroform-*d* or THF-$d_8$ as the solvent, and the chemical shifts are reported on the $\delta$ scale using tetramethylsilane (TMS) as the internal reference. The UV/vis spectra were recorded on a Milton Roy Spectronic 3000 array spectrometer, and the MS analysis was carried out on a Finnigan TSQ 7000 triple quadrupole mass spectrometer operating in an electron impact (EI) mode. The TGA analysis was performed on a Perkin-Elmer TGA 7 under nitrogen at a heating rate of 20 °C/min, and the DSC thermograms were recorded on a Setaram DSC 92 at a heating or cooling rate of 10 °C/min. An Olympus BX 60 POM equipped with a Linkam TMS 92 hot stage was used for the optical texture observation.

The molecular weights of **2** were estimated by a GPC system consisting of a Waters 510 HPLC pump, a Rheodyne 7725i injector with a stand kit, a set of Styragel columns (HT3, HT4, and HT6; molecular weight range, $10^2$−$10^7$), a column temperature controller, a Waters 486 wavelength-tunable UV/vis detector, a Waters 410 differential refractometer, and a system DMM/scanner with an 8-channel scanner option. THF was used as the eluent, and the flow rate was 1.0 mL/min. The column temperature was maintained at 40 °C, and the working wavelength of the UV detector was set at 254 nm. A set of 12 monodisperse polystyrene standards (Waters) was used for the molecular weight calibration.

The XRD patterns were recorded on a Philips PW 1830 powder diffractometer at room temperature using the monochromatized X-ray beam from the nickel-filtered Cu *K*α radiation with a wavelength of 1.5406 Å (scan rate, 0.01°/s; scan range, 2−30°). The samples for the XRD experiments were prepared by quickly quenching by liquid nitrogen the polymers annealed at their liquid crystalline states.[12] A typical experimental procedure for the sample preparation is given

(38) Group dipole moments ($10^{18}$ esu): CN, 4.0; MeO, 1.3.[39] Obviously, compared to the methoxy tails, the cyano tails can polarize the mesogenic pendants to a much larger extent.

(39) (a) Carey, F. A.; Sundberg, R. J. *Advanced Organic Chemistry*, 3rd ed.; Plenum Press: New York, 1990. (b) Smyth, C. P. *Dielectric Behaviour and Structure*; McGraw-Hill: New York, 1955.

(40) (a) Zhou, Q.; Wan, X.; Zhang, F.; Zhang, D.; Wu, Z.; Feng, X. *Liq. Cryst.* **1993**, *13*, 851. (b) Song, W.; Chen, S.; Qian, R. *Makromol. Chem., Rapid Commun.* **1993**, *14*, 605. (c) Witteler, H.; Lieser, G.; Wegner, G.; Schulze, M. *Makromol. Chem., Rapid Commun.* **1993**, *14*, 471. (d) Gali, G.; Laus, M.; Angelou, A. S.; Ferruti, P.; Chiellini, E. *Eur. Polym. J.* **1985**, *21*, 727.

(41) (a) Petty, M. C.; Bryce, M. R.; Bloor, D. *An Introduction to Molecular Electronics*; Edward Arnold: London, 1995. (b) *Conjugated Polymers and Related Materials: the Interconnection of Chemical and Electronic Structure*; Salaneck, W. R., Lunstrom, I., Ranby, B., Eds.; Oxford University Press: Oxford, U.K., 1993. (c) *Conjugated Polymers: the Novel Science and Technology of Highly Conducting and Nonlinear Optically Active Materials*; Bredas, J. L., Silbey, R., Eds.; Kluwer Academic Publishers: Dordrecht, The Netherlands, 1991. (d) *Electronic and Photonic Applications of Polymers*; Bowden, M. J., Turner, S. R., Eds.; American Chemical Society: Washington, DC, 1988.

below: A film of **2a** cast on a single-crystal silicon wafer was heated on the hot stage to its isotropic state (215 °C), at which the sample was annealed for 5 min. After being cooled at a rate of 10 °C/min to its liquid crystalline state (165 °C) and annealed there for 5 min, the wafer was thrown into a liquid nitrogen Dewar flask. The wafer was taken out from the flask and naturally warmed to room temperature. The film thus obtained on the wafer was then used for the XRD measurement.

**Synthesis of (((4-carboxyphenyl)oxy)carbonyl)-1-decyne.** Into a 100-mL two-necked flask equipped with a reflux condenser were added 10-undecynoic acid (4.56 g, 0.025 mol), THF (25 mL), and thionyl chloride (4 mL) under a dry nitrogen atmosphere. After the solution was refluxed for 2 h, THF and thionyl chloride were removed under reduced pressure at room temperature. The residue was dissolved in 25 mL of THF and cooled to 0−5 °C by an ice bath. 4-Hydroxybenzoic acid (2.76 g, 0.02 mol) and pyridine (4 mL) in 25 mL of THF were then added into the flask under nitrogen. After the reaction mixture was stirred for 6 h, the volatiles were removed by a rotary evaporator. The residue was recrystallized in an ethanol−water mixture, and 5.0 g of the product was obtained as white crystals after drying in a vacuum oven at 50 °C (yield: 82.7%). IR (KBr, $\nu$): 3290 (≡C−H), 2120 (C≡C), 1754 ($CO_2Ar$), 1684 ($CO_2H$) $cm^{-1}$. $^1H$ NMR (300 MHz, $CDCl_3$, TMS, ppm): $\delta$ 8.16 (m, 2H, Ar H), 7.22 (m, 2H, Ar H), 2.58 (t, 2H, $CH_2CO_2$), 2.19 (dt, 2H, $CH_2C{\equiv}C$), 1.94 (t, 1H, C≡CH), 1.76 (quintet, 2H, $CH_2CH_2CO_2$), 1.54 (quintet, 2H, $CH_2CH_2C{\equiv}C$), 1.42−1.36 [m, 8H, $(CH_2)_4$]. $^{13}C$ NMR (75 MHz, $CDCl_3$, TMS, ppm): $\delta$ 171.6 ($CO_2Ar$), 171.4 ($CO_2H$), 155.1, 131.8, 126.7, 121.7 (aromatic carbons), 84.7 (*C*≡CH), 68.1 (C≡*C*H), 34.3 ($CH_2CO_2$), 29.1, 29.0, 28.9, 28.6, 28.4 [$(CH_2)_5$], 24.8 ($CH_2CH_2CO_2$), 18.4 ($CH_2C{\equiv}C$).

**Synthesis of 10-[(4-((4′-Cyanophenoxy)carbonyl)-phenoxy)carbonyl]-1-decyne (1a).** In a 250-mL flask were placed 1.21 g (4 mmol) of ((4-carboxyphenoxy)carbonyl)-1-decyne, 0.524 g (4.4 mmol) of 4-cyanophenol, 0.99 g (4.8 mmol) of DCC, and 0.049 g (0.4 mmol) of DMAP. The contents were dissolved in 180 mL of methylene chloride, and the resulting solution was stirred for 12 h at room temperature under nitrogen. The crystalline urea byproduct was then filtered out from the reaction mixture, and the solvent of the filtrate was evaporated. The residue was purified by a silica gel column using chloroform as the eluent. After recrystallization in ethanol, 0.87 g of **1a** was obtained as needlelike white crystals in yield 53.9%. IR (KBr, $\nu$): 3260 (≡C−H), 2234 (C≡N), 1760 ($CH_2CO_2Ar$), 1740 ($ArCO_2Ar$), 698 (≡C−H), 684 (≡C−H) $cm^{-1}$. $^1H$ NMR (300 MHz, $CDCl_3$, TMS, ppm): $\delta$ 8.21 (m, 2H, Ar H), 7.75 (m, 2H, Ar H), 7.37 (m, 2H, Ar H), 7.26 (m, 2H, Ar H), 2.60 (t, 2H, $CH_2CO_2$), 2.20 (dt, 2H, $CH_2C{\equiv}C$), 1.95 (t, 1H, C≡CH), 1.78 (quintet, 2H, $CH_2CH_2CO_2$), 1.54 (quintet, 2H, $CH_2CH_2C{\equiv}C$), 1.44−1.36 [m, 8H, $(CH_2)_4$]. $^{13}C$ NMR (75 MHz, $CDCl_3$, TMS, ppm): $\delta$ 171.5 ($CO_2$), 155.4, 154.1, 133.7, 131.9, 126.0, 122.9, 122.1, 109.9 (aromatic carbons), 118.2 (CN), 84.6 (*C*≡CH), 68.1 (C≡*C*H), 34.3 ($CH_2CO_2$), 29.1, 29.0, 28.9, 28.6, 28.4 [$(CH_2)_5$], 24.7 ($CH_2CH_2CO_2$), 18.4 ($CH_2C{\equiv}C$). MS (EI): *m*/*z* 285.2 {$[M - (OC_6H_4CN)]^+$, calcd 285.2}, 165.2 {$[M - (OC_6H_4CO_2C_6H_4CN)]^+$, calcd 165.2}.

**Synthesis of 10-[(4-((4′-Methoxyphenoxy)carbonyl)-phenoxy)carbonyl]-1-decyne (1b).** The experimental procedure is similar to that described above for the synthesis of **1a** with production of flaky white crystals in yield 34.9%. IR (KBr, $\nu$): 3286 (≡C−H), 1752 ($CH_2CO_2Ar$), 1744 ($ArCO_2Ar$), 686 (≡C−H), 632 (≡C−H) $cm^{-1}$. $^1H$ NMR (300 MHz, $CDCl_3$, TMS, ppm): $\delta$ 8.21 (m, 2H, Ar H), 7.24 (m, 2H, Ar H), 7.13 (m, 2H, Ar H), 6.95 (m, 2H, Ar H), 3.82 (s, 3H, $OCH_3$), 2.59 (t, 2H, $CH_2CO_2$), 2.20 (dt, 2H, $CH_2C{\equiv}C$), 1.95 (t, 1H, C≡CH), 1.77 (quintet, 2H, $CH_2CH_2CO_2$), 1.54 (quintet, 2H, $CH_2CH_2C{\equiv}C$), 1.44−1.36 [m, 8H, $(CH_2)_4$]. $^{13}C$ NMR (75 MHz, $CDCl_3$, TMS, ppm): $\delta$ 171.6 ($CO_2$), 157.3, 154.9, 144.3, 131.7, 127.0, 122.4, 121.8, 114.5 (aromatic carbons), 84.7 (*C*≡CH), 68.1 (C≡*C*H), 55.6 ($OCH_3$), 34.4 ($CH_2CO_2$), 29.1, 29.0, 28.9, 28.6, 28.4 [$(CH_2)_5$], 24.8 ($CH_2CH_2CO_2$), 18.4 ($CH_2C{\equiv}C$). MS (EI): *m*/*z* 408.2 ($M^+$, calcd 408.2), 285.2 {$[M - (OC_6H_4OCH_3)]^+$, calcd 285.2}.

**Synthesis of Poly{10-[(4-((4′-cyanophenoxy)carbonyl)-phenoxy)carbonyl]-1-decyne} (2a).** Into a baked 20-mL Schlenk tube with a three-way stopcock on the side arm was added 323 mg of **1a**. The tube was evacuated under vacuum and then flushed with dry nitrogen through the side arm; the procedure was repeated three times to remove air/moisture trapped, if any, inside the crystalline monomer. Freshly distilled dioxane (2 mL) was then injected into the tube through a septum to dissolve the monomer. The $WCl_6-Ph_4Sn$/dioxane complex was prepared in another Schlenk tube by dissolving 15.9 mg of $WCl_6$ and 17.1 mg of $Ph_4Sn$ in 2 mL of dioxane. After aging at room temperature for 10 min, the homogeneous complex solution was transferred to the monomer solution by a hydrodermic syringe. The resulting mixture was stirred under nitrogen at room temperature for 24 h and was then diluted with 5 mL of dioxane. The dilute polymer solution was added dropwise to 200 mL of methanol through a cotton filter with stirring. The precipitate was allowed to stand overnight, which was then filtered out by a Pyrex Gooch crucible, washed with methanol, and dried in a vacuum oven at 40 °C to a constant weight. The isolated polymer was further purified by reprecipitation of its dioxane solution into ether to give yellow powders in yield 46.8%. $M_w$ = 29 000; $M_w/M_n$ = 1.7 (GPC, polystyrene calibration). IR (KBr, $\nu$): 2232 (C≡N), 1740 ($CO_2R$) $cm^{-1}$. $^1H$ NMR (300 MHz, THF-$d_8$, TMS, ppm): $\delta$ 8.21, 7.83, 7.47, 7.33 (Ar H, trans HC=C), 6.07 (cis HC=C), 2.67 ($CH_2CO_2$), 2.35 ($CH_2C{=}C$), 1.85 ($CH_2CH_2CO_2$), 1.51 [$(CH_2)_5$]. $^{13}C$ NMR (75 MHz, THF-$d_8$, TMS, ppm): $\delta$ 174.3, 171.3, 163.4, 155.2, 154.0, 133.7, 131.8, 126.1, 122.8, 122.0, 118.1, 110.0, 34.3, 29.3, 24.8. UV/vis (THF): $\lambda_{max}(\epsilon)$ 243 nm (31 600 $g^{-1}$ mL $cm^{-1}$).

**Synthesis of Poly{10-[(4-((4′-methoxyphenoxy)carbonyl)phenoxy)carbonyl]-1-decyne} (2b).** The polymerization procedure is similar to that detailed above: yellow powders; yield 35.3%; $M_w$ = 28 400; $M_w/M_n$ = 2.6 (GPC, polystyrene calibration). IR (KBr, $\nu$): 1758 ($CH_2CO_2Ar$), 1736 ($ArCO_2Ar$) $cm^{-1}$. $^1H$ NMR (300 MHz, $CDCl_3$, TMS, ppm): $\delta$ 8.21, 7.14, 7.02, 6.85 (Ar H, trans HC=C), 5.87 (cis HC=C), 3.75 ($CH_3O$), 2.51 ($CH_2CO_2$), 2.20 ($CH_2C{=}C$), 1.71 ($CH_2CH_2CO_2$), 1.36 [$(CH_2)_5$]. UV/vis (THF): $\lambda_{max}(\epsilon)$ 237 (18 600), 276 (7080) nm ($g^{-1}$ mL $cm^{-1}$).

**Acknowledgment.** We thank the financial support provided by the Hong Kong Research Grants Council through the Earmarked Research Grants HKUST597/95P and HKUST6149/97P. This project also benefited from the support of the Hong Kong Industry Department, the Nanostructure Materials and Technology Joint Laboratory of Hong Kong University of Science & Technology (HKUST) and Chinese Academy of Sciences, the Advanced Materials Research Institute of HKUST, and the Technology Resource International Corp., Alpharetta, GA.

CM9803152